ELSEVIER

Polymer 42 (2001) 6793–6800

polymer

www.elsevier.nl/locate/polymer

Dielectric properties of poly(triethylene glycol *p*,*p*′-bibenzoate-*co*-(*R*)-(+)3-methyl adipate)

Abel Garcia-Bernabé[a], Ricardo Díaz-Calleja[a,*], Antonio Bello[b], Ernesto Pérez[b]

[a]*Departamento de Termodinámica Aplicada, Universidad Politécnica de Valencia, ETSII (UPV), Camino de Vera, Apartado 22012, 46022 Valencia, Spain*
[b]*Departamento de Química-Física, Instituto de Ciencia y Tecnología de Polímeros, CSIC, Madrid, Spain*

Received 22 January 2001; accepted 5 February 2001

Abstract

In this study, a copolyester of poly(triethylene glycol *p*,*p*′-bibenzoate-*co*-(*R*)-3-methyl adipate) was prepared. The mesophase texture, the thermal and dielectric properties (a.c.-dynamical as well as thermostimulated depolarization currents) were studied. X-ray diffractograms reveal a relatively stable mesophase smectic S_c, whereas DSC shows on heating only the glass transition and the endotherm due the isotropization of the mesophase. Dynamic dielectric measurements show a broad sub-T_g relaxation together with an α loss peak (associated with the glass transition) overlapped with a significant conductive contribution. After separating this contribution from the dipolar component of the dielectric loss, we have modeled the relaxation according to classical empirical models. Thermostimulated depolarization currents also show three relaxations. The fine structure of these relaxations is analyzed by the thermal sampling technique.

Keywords: Copolyester; Smectic mesophase; Dielectric relaxation

1. Introduction

In previous papers [1,2], some properties of poly(triethylene glycol *p*,*p*′-bibenzoate) (PTEB) were reported. This polymer develops a smectic structure with the long chains parallel but with a tilt angle with respect to the smectic layer. On the basis of the X-ray diffractogram the mesophase was classified as smectic S_c. This kind of mesophase is particularly interesting, since by introducing chiral centres into the structures may develop mesophases with ferroelectric properties [3].

It is well-known that dielectric spectroscopy is a convenient tool for analyzing the structure and properties of polymer liquid crystals. For example, in materials developing smectic structures as ferroelectric liquid crystals, Kremer and others [4] have described a complex dielectric behaviour for unaligned and for aligned polymers in terms of the chiral S_c phase, namely Goldstone and soft mode, respectively.

We have synthesized several copolyesters of triethylene glycol with ethyl *p*,*p*′-bibenzoate (BB) and *R*(+) 3-methyl adipate (DMA). In this paper, we report on the characterization and dielectric behaviour, a.c. and TSDC, of one of these copolymers, with a very small amount of DMA (the proportion of BB/DMA is 15:1). The experimental data show indication of a phase change near 70°C together with well-developed β, α and conductive relaxations.

2. Experimental section

Materials. 4,4′-Biphenyldicarboxylic acid (97%, Aldrich), (*R*)(+)3-methyladipic acid, $[\alpha] = +7.2$ (96%, Aldrich), triethylenglycol (99%, Fluka).

Synthesis. The polymer was synthesized by melt polycondensation. Transesterification was carried out using diethyl *p*,*p*′-bibenzoate (BB) and (*R*)(+) diethyl 3-methyl adipate (DMA) with molar ratio 15:1, and triethylene glycol, using isopropyl titanate as catalyst. The polyester, CTRBMA-1, was purified by pouring into methanol a solution of the polymer in chloroform. After drying, the polymer exhibits a brown colour that becomes red for samples with a composition in which the proportion of BB/DMA is 7:1. In this work, only the copolymer with composition BB/DMA, 15:1 was used.

Characterization. The thermal properties of these samples were measured with a Perkin–Elmer DSC-7 calorimeter interfaced to a data station. Wide angle X-ray diffractions of samples, freshly cooled from the melt and stretched

* Corresponding author. Tel.: +34-9-6387-7320; fax: +34-9-6387-7329.
E-mail address: rdiazc@ter.upv.es (R. Díaz-Calleja).

0032-3861/01/$ - see front matter
PII: S0032-3861(01)00141-0

to a draw ratio of about 10:1, were taken with a sample film distance of 60 mm. Nickel filtered, CuKα radiation was used.

Dielectric permittivity measurements were carried out using a TA dielectric analyzer (DEA 2970) between −120 and 100°C in a range of frequencies from 0.1 to 3×10^4 Hz. Pill-shaped samples were pressed between gold parallel plate electrodes at 100°C prior to measurements in order to ensure good electrical contact.

Thermostimulated depolarization current, TSDC, experiments were carried out by a TSC/RMA instrument (Solomat). A global spectrum was obtained by polarization at 100°C by a 5×10^5 kV m^{-1} during 2 min in a 0.5 m m^{-1} thickness sample with 78 mm^2 of area. After quenching to −120°C, TSD currents were collected at a rate of 7°C/min until 100°C. In order to analyze the fine structure of the relaxation peaks, partial depolarizations were carried out by the thermal sampling method in the low temperature peak zone between −120 and −70°C for polarization temperature, T_p, and a temperature window of 10°C for subglass relaxation, and from 10 to 40°C in 5°C steps for the relaxation associated to the glass transition. In all the cases, the rate of heating was also 7°C/min and the starting and finishing temperatures for each partial depolarization were $T_p = -30$°C and $T_p = +40$°C. The electric field for the polarization was also 5×10^5 kV m^{-1}.

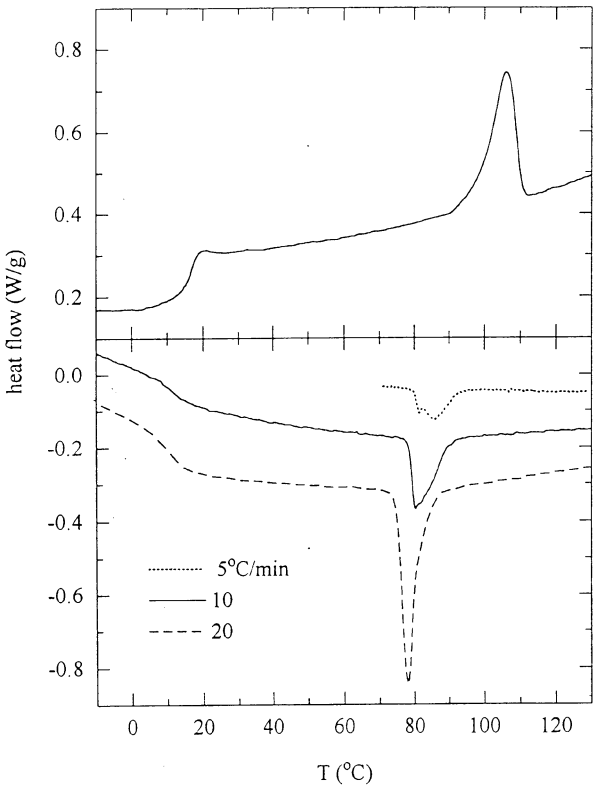

Fig. 1. DSC cooling curves from the melt at the indicated rates (lower) and subsequent heating (upper) at 10°C/min.

3. Results and discussion

3.1. Phase behaviour

DSC scans for the copolymer CTRBMA-1 are given in Fig. 1. Starting from the melt state at 150°C and cooling the sample, the thermograms show bimodal exothermic peaks that depend on the cooling rate (lower part of Fig. 1). The subsequent heating of the sample shows the glass transition and a broad endotherm with a maximum at 104°C (upper part of Fig. 1). The nature of this transition corresponds to a smectic-isotropic change. The reason of the bimodal character of the exothermic peak observed on cooling only at low rates, is not known but probably is due to the polydispersity that introduces the heterogeneous composition of the copolymer. The enthalpy and entropy associated with this process are 0.72 kcal mol^{-1} and 1.9 cal mol^{-1}K^{-1}, respectively.

Comparing these values with those published for PTEB (1) one arrives to the conclusion that all the thermodynamic parameters involved in this transition for the copolymer (CTRBMA-1), like enthalpy and entropy, have a lower value, about 20% for the entropy and 15% for the enthalpy in relation to the homopolymer PTEB.

Concerning to the stability of the mesophase, the copolymer can be held a room temperature, as happens with the PTEB, several days without detecting any transformation to a crystalline phase.

Therefore, the copolymerization of PTEB with a tiny amount of the chiral compound (DMA) affects more to the thermodynamic parameters of the transformation than to the stability of the mesophase.

Mesophase structure. All the X-ray diffractograms were done at room temperature with the sample recently quenched from the melt state to room temperature. In these experimental conditions, the X-ray diffractions of the isotropic sample CTRBMA-1 are consistent with a smectic phase. The diffractogram shows three rings: the broad outer halo at $2\theta = 20.1°$, corresponding to the intermolecular distance of 4.4 Å, an inner ring at a spacing of 18.5 Å, due to the repeating period of the smectic layer, and its second order. The stretched sample exhibits the broad outer reflection with the maximum of intensity centered on the equator, whereas the inner reflection is divided into four spots out of the meridional one in each quadrant, Fig. 2. The spots form a finite angle with the chain molecular axis and no layer reflections appear on the meridional line for this smectic phase. This behaviour, in which the chain is tilted with respect to the layers, corresponds to the accepted structure for the S_c mesophase. The tilt angle of the chain molecule with respect to the

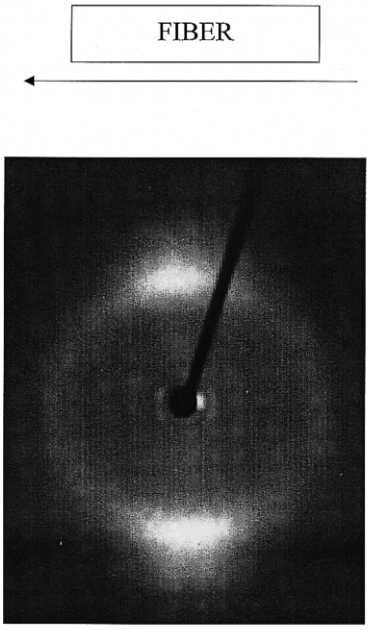

Fig. 2. X-ray photograph observed for the copolymer fiber.

normal to the smectic layers is about 20°. The mesophase structure of this copolymer does not show appreciable differences with that of PTEB (1).

3.1.1. Dielectric a.c. data

In Fig. 3, we can see the dielectric loss of this polymer as a function of temperature at several frequencies. A first inspection of the data reveals a broad secondary relaxation peak extending from −120 to 0°C. A careful revision of the data seems to show two overlapped peaks.

From 0 to 50°C we observe a prominent α relaxation. Its position and intensity allows us to identify it with the glass-transition of the polymer. The value of T_g found from DSC is 16°C (see Fig. 1). A rapid increase of the loss is observed

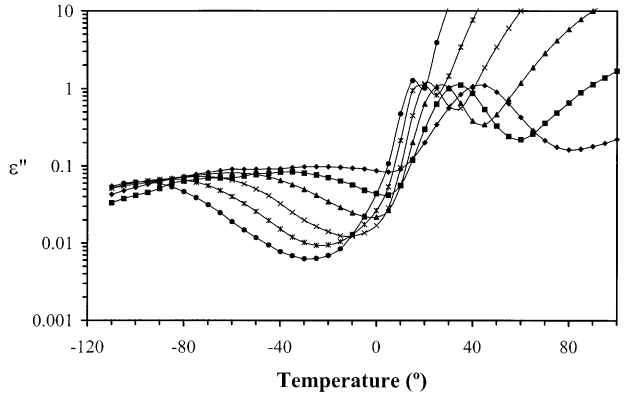

Fig. 3. Dielectric loss permittivity of CTRBMA-1. 3×10^4 Hz (◆), 3×10^3 Hz (■), 3×10^2 Hz (▲), 30 Hz (×), 3 Hz (∗), 0.3 Hz (●).

above this temperature as is common in other polymers. We now discuss separately each relaxation.

The low temperature relaxation peak, which will be called β, is strongly asymmetric. This situation is similar to that observed by Kremer and co-workers in a relatively similar system [4]. Thus, we can tentatively attribute the low temperature side (β_s peak) to motions of the glycol residue and the high temperature side (β_m peak) to rotational motions of mesogenic (biphenyl) groups. In this respect, it is interesting to note that the β_m peak has an activation energy of 58 kJ mol^{-1}, that is similar to the β relaxation of polyethylene terephtalate (PET) reported by Illers and Breuer [5] (54 kJ mol^{-1}), which they attribute to rotational motion of ester residue.

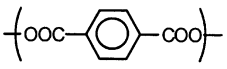

As we have mentioned before with regard to the α relaxation, we observe overlapping of the conductive (and probably interfacial) effects with the typical α dipolar relaxation. This situation is also found in many other polymer systems [6].

It is informative to represent the dielectric data in terms of the dielectric modulus, M^*, instead of the dielectric permittivity, ϵ^*. This quantity is defined as

$$M^* = (\epsilon^*)^{-1} \tag{1}$$

and consequently

$$M'' = \mathrm{Im}(M^*) = \frac{\epsilon''}{|\epsilon^*|^2}, \tag{2}$$

where $|\epsilon^*| = (\epsilon'^2 + \epsilon''^2)^{1/2}$.

In Fig. 4, we can see the dielectric loss modulus of CTRBMA-1 between about 10 and 90°C at 0.1, 0.3, 1 and 3 Hz. Two main peaks are seen. The low temperature one corresponds to the α dipolar relaxation whereas the high temperature peak is due to the conductive effects in the bulk and other effects presumably related to the blocked electrodes. Fig. 5 presents log M' and log(tan δ) as a function of the temperature for the same four frequencies. The presence of three relaxations is clearly observed. The breaking of the trend in tan δ and the inflection in log M' at about 70°C indicates a significative modification of the material that can be correlated with DSC data.

In order to separate dipolar contribution to the loss from other ones it is convenient to return to a log ϵ'' vs. log f representation (see Fig. 6). Here we observe the typical trend of log ϵ'' at low frequencies. In this regime, we find a ω^{-1} dependence of ϵ''. The equivalent electrical assembly for this behaviour is a circuit consisting of a resistance with a capacitance in parallel, and as it is well-known

$$\sigma = \epsilon'' \omega \epsilon, \tag{3}$$

where σ represents the conductivity, ω is the angular

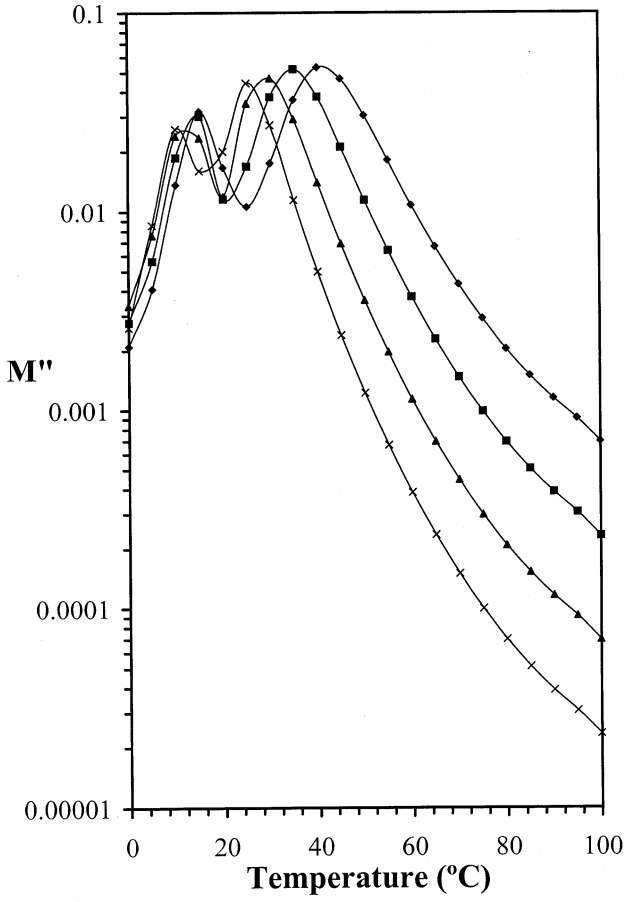

Fig. 4. Dielectric loss modulus for CTRBMA-1. 3 Hz (◆), 1 Hz (■), 0.3 Hz (▲), 0.1 (×).

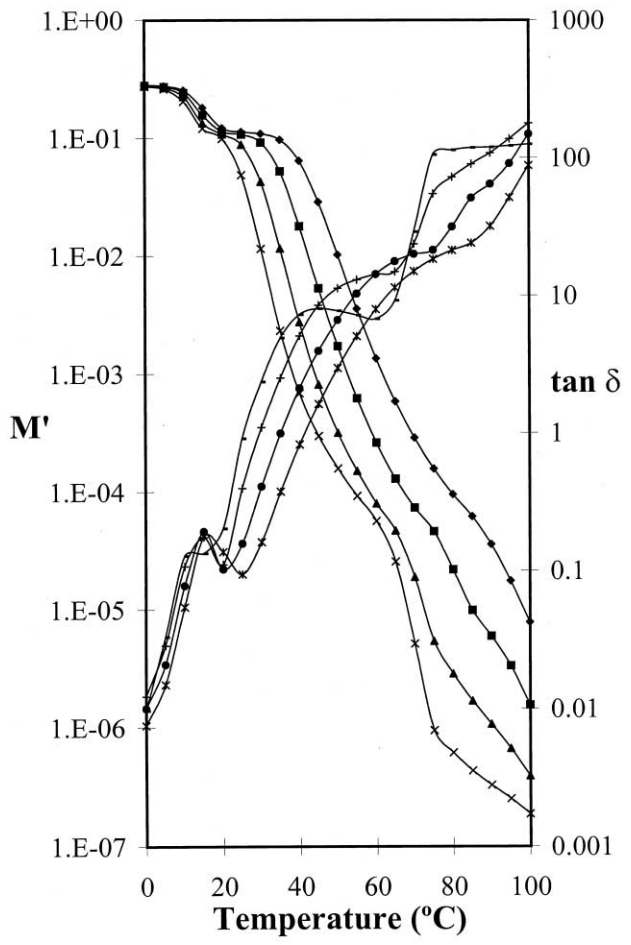

Fig. 5. Dielectric modulus and tan δ as a function of the temperature. 3 Hz (◆), 1 Hz (■), 0.3 Hz (▲), 0.1 (×) for dielectric modulus and 3 Hz (∗), 1 Hz (●), 0.3 Hz (+), 0.1 Hz (−) for tan δ.

frequency and ϵ is the permittivity of free space. The values obtained for the conductivity with respect to the temperature are compiled in Table 1. The activation energy of the conductivity is obtained from a plot of Ln σ against T^{-1} (Fig. 7). This representation shows two characteristic zones, with activation energies of 106.8 and 59.7 kJ mol^{-1} for the low and high temperature zones, respectively, with a crossover at about 70°C. This is an indication that an important structural modification has occurred in the polymer at this temperature.

By assuming a −1 slope behaviour for the conductivity, by subtraction we can have new curves. The trend of these curves at low frequency seems to show the presence of a new conductive phenomenon probably related to the electrode blocking. At relatively low temperatures (20–30°C) these effects are not very important. The α relaxation can be represented by the skewed Havriliak–Negami [7] model in this temperature range

$$\epsilon^*(\omega) = \epsilon_\infty + \frac{\epsilon_0 - \epsilon_\infty}{(1 + (j\omega\tau)^\alpha)^\beta}, \tag{4}$$

where ϵ_0 and ϵ_∞ are, respectively, the relaxed and unrelaxed dielectric permittivities, τ the relaxation time and α and β are the parameters related to the shape and skewness of the complex dielectric plot. The parameters of this model were obtained by means of the LEVM6 [8] program. The values obtained at 25°C are 8.62 for ϵ_0, 3.45 for ϵ_∞, 2.32×10^{-2} s for relaxation time, 0.72 for α and 0.41 for β.

As is well known [9], the frequency-dependent complex permittivity ϵ^* is related to the dipolar correlation function

Table 1
Conductivity of CTRBMA-1

T (°C)	σ (S m^{-1})	T (°C)	σ (S m^{-1})
100	2.23×10^{-7}	65	2.33×10^{-8}
95	1.72×10^{-7}	60	1.42×10^{-8}
90	1.37×10^{-7}	55	8.15×10^{-9}
85	1.06×10^{-7}	50	4.50×10^{-9}
80	7.80×10^{-8}	45	2.33×10^{-9}
75	5.45×10^{-8}	40	1.11×10^{-9}
70	3.63×10^{-8}	35	6.23×10^{-10}

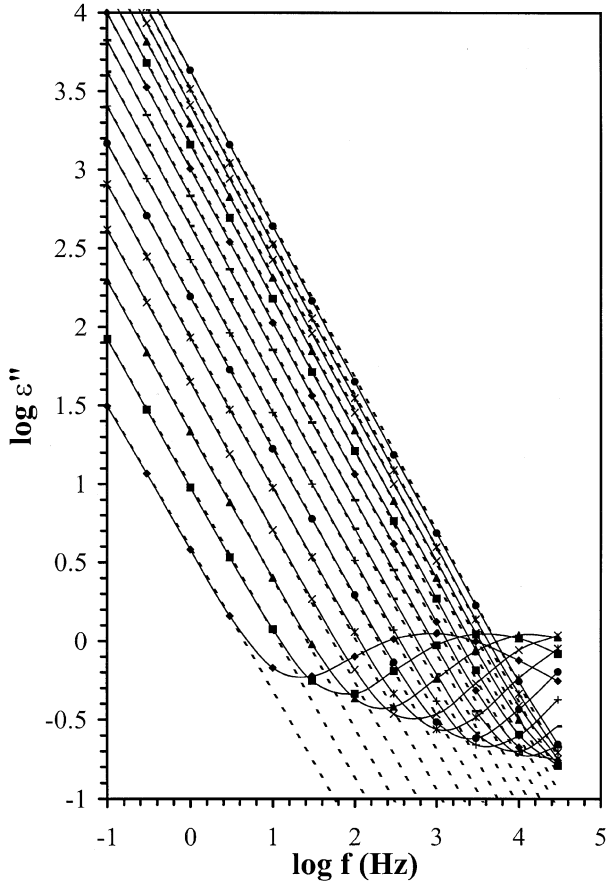

Fig. 6. Log ϵ'' vs. log f. 30°C (◆), 35°C (■), 40°C (▲), 45°C (×), 50°C (∗), 55°C (●), 60°C (+), 65°C (−), 70°C (—), 75°C (◆), 80°C (■), 85°C (▲), 90°C (×), 95°C (∗), 100°C (●).

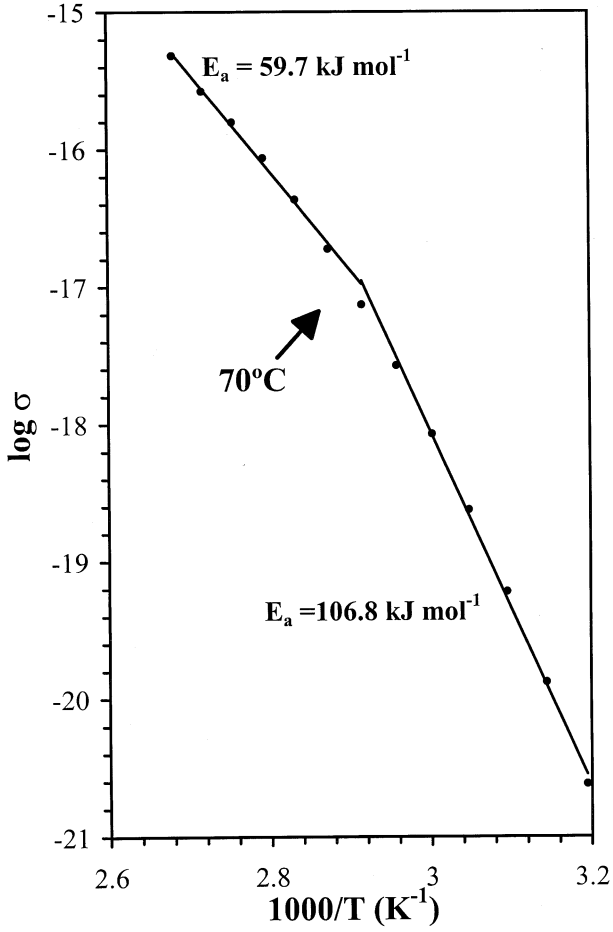

Fig. 7. Log ϵ'' vs. $10^3/T$ plot showing two characteristic zones.

$\Phi_{(t)}$ by means of

$$\frac{\epsilon^* - \epsilon_\infty}{\epsilon_0 - \epsilon_\infty} = \int_0^\infty \exp(j\omega t)(-\Phi(t)\ \partial t, \tag{5}$$

where ϵ_0 and ϵ_∞ are the low and high frequency permittivities. The total dipole correlation function is given by

$$\Phi(t) = \frac{\sum_i^N \sum_j^N \langle \mu_i(0)\mu_j(t)\rangle}{\sum_i^N \sum_j^N \langle \mu_i(0)\mu_j(0)\rangle,} \tag{6}$$

where μ_i are the dipole moments in the chains.

We can obtain the macroscopic correlation function by Fourier inversion of Eq. (5). Thus assuming the cosine transformation, we have

$$\Phi(t) = \frac{2}{\pi}\int_0^\infty \frac{\epsilon''(\omega)}{\epsilon_0 - \epsilon_\infty}\frac{\cos\omega t}{\omega}\ \partial t. \tag{7}$$

The real and imaginary parts of ϵ^* are related through Kramers–Kronig relationships, so we can perform the calculation of $\Phi(t)$ via ϵ' (sine transformation) also via ϵ'' (cosine transformation) as in our case.

For $\epsilon''(\omega)$ in Eq. (7) we can use the following expressions obtained from the Havriliak–Negami (H–N) equation:

$$\epsilon''(\omega) = (\epsilon_0 - \epsilon_\infty)\gamma^{-\beta'}\sin\beta'\theta, \tag{8}$$

$$\gamma = \left[1 + 2(\omega\tau)^\alpha \cos\left(\frac{\alpha\pi}{2}\right) + (\omega\tau)^{2\alpha}\right]^{1/2}, \tag{9}$$

$$\theta = \arctan\frac{(\omega\tau)^\alpha \sin\left(\alpha\frac{\pi}{2}\right)}{1 + (\omega\tau)^\alpha \cos\left(\alpha\frac{\pi}{2}\right)}. \tag{10}$$

The result of the transformation can be expressed in terms of a KWW equation [8]. The data from the H–N equation are used to obtain $\phi(t)$ (Fig. 8) with $\tau_\kappa = 1.08\times10^{-2}$ s and $\beta = 0.404$, where τ_κ is related to a retardation time by means of

$$\log\langle\tau\rangle = \frac{1}{\ln 10}\ln\left[\frac{\tau_\kappa}{\beta}\Gamma\left(\frac{1}{\beta}\right)\right] \tag{11}$$

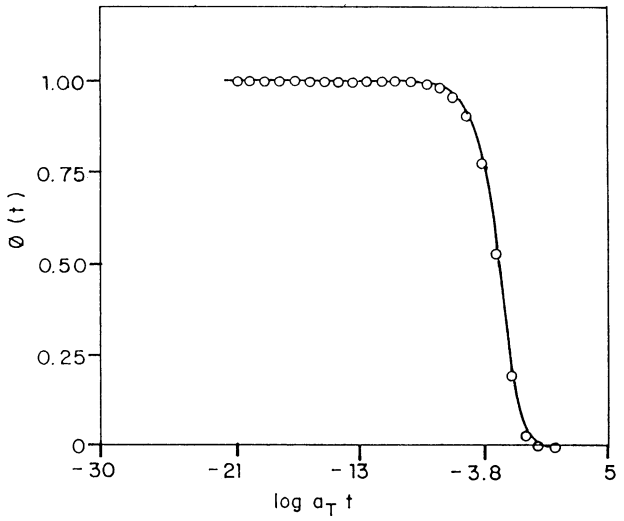

Fig. 8. Correlation function for the α process at 20°C.

and Γ is the gamma function. From the last equation we have $\langle\tau\rangle = 3.5 \times 10^{-2}$ s. We emphasize that the value obtained for β (= 0.404) is close to that obtained for similar α-dipolar relaxations in polymers.

The α relaxation in the frequency domain can be conveniently analyzed by means the Vogel–Fulcher–Tamman–Hesse (VFTH) equation [10,11,12] formulated empirically by these authors as

$$Ln(f_{max}) = A - \frac{m}{T - T_\infty}, \tag{12}$$

where A and m are constants. T_∞ is the temperature where the redistribution energy will be large and free volume is practically zero. In this case, the values of T_∞ obtained is −43°C and the value of m amounts to 2106.

The Doolittle equation (13) relates the free volume (ϕ/B) with de value of m in the VFTH relationship. The free volume at T_g(ϕ_g/B) is 2.8%, in relatively good agreement with the free volume theory

$$\frac{\phi}{B} = \frac{T - T_\infty}{m}. \tag{13}$$

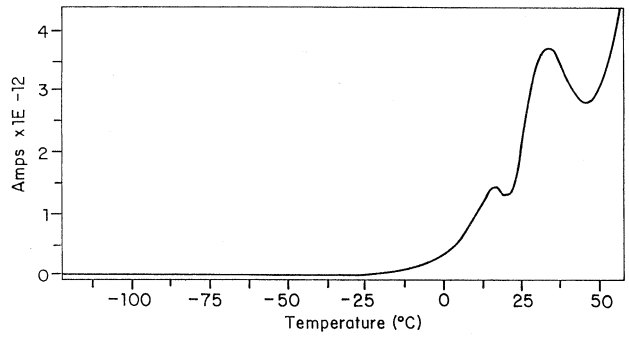

Fig. 9. TDSC full spectrum of CTRBMA-1. Polarization temperature 100°C. (Experimental details are given in Section 2.)

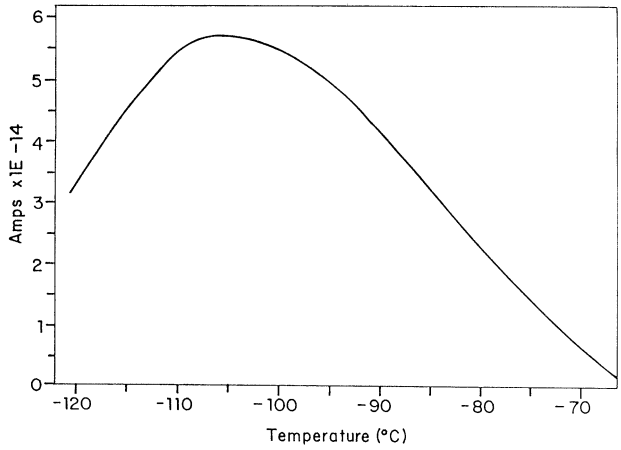

Fig. 10. Low temperature peak of CTRBMA-1.

3.1.2. Thermostimulated depolarization currents

TSDC measurements have been performed in two ways: first we have obtained the global spectrum (see Fig. 9) in which can be observed (see inset) a low temperature peak near −105°C (Fig. 10) assigned to the β dielectric relaxation, and two peaks, at about 15 and 30°C. The lower temperature peak may be due to the α dipolar relaxation and the higher temperature peak is probably due to space charge as is commonly found in many polymer systems. At higher temperatures the current increases continuously. In order to analyze more carefully the low temperature peak and the room temperature zone we have carried out partial depolarizations according to the thermal sampling technique (see Section 2). Results are shown in Figs. 11 and 12.

In Fig. 11 we see that in the third depolarization curve (with $T_p = 20$°C) there is overlap between the dipolar α-peak and the free charges peak. Above 35°C the resolution of the peaks is bad due to the continuous increase of the current in this zone. From the partial relaxation peaks we

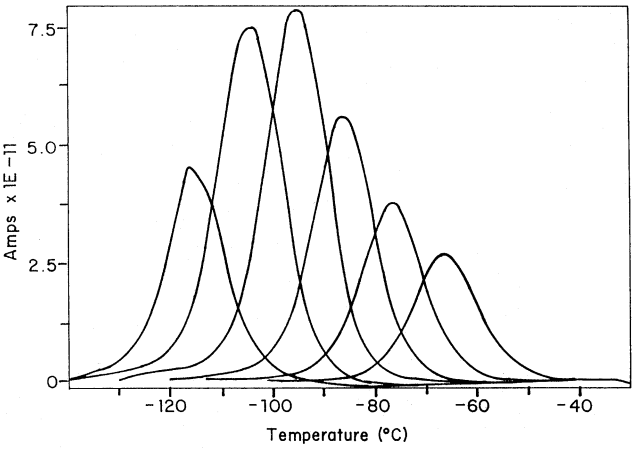

Fig. 11. Partial depolarization for the subglass relaxation process. Polarization temperatures are −120, −110, −100, −90, −80, and −70°C for the respective curves in the increasing temperature sense.

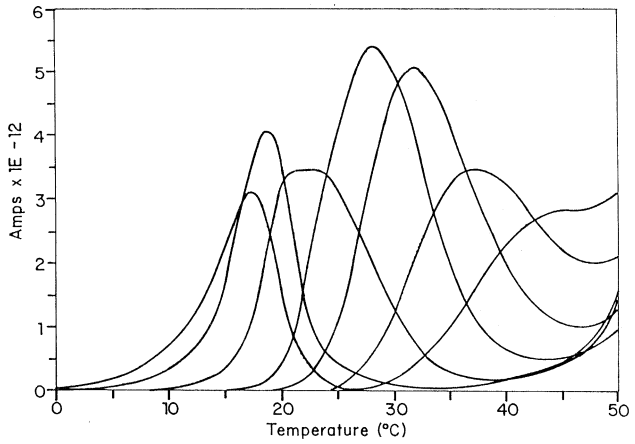

Fig. 12. Partial depolarization in the room temperature region (α and ρ peaks). Polarization temperatures: 10, 15, 20, 25, 30, 35 and 40°C.

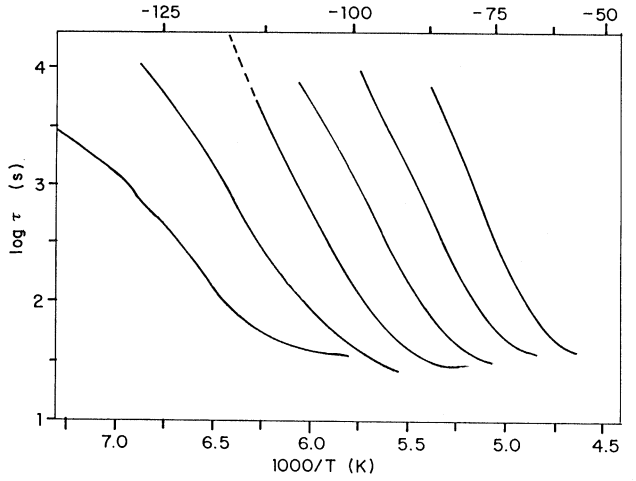

Fig. 13. Arrhenius plot for the six relaxation peaks in Fig. 10 (the corresponding activation parameters are listed in Table 1).

obtain the relaxation time according to the following equation:

$$\tau(T) = \frac{\int_{T_{in}}^{T} i(T)(\partial t/\partial T)\,\partial T}{i(T)}, \tag{14}$$

where $\partial t/\partial T$ represents the reciprocal of the heating rate, $i(T)$ the current and T_{in} is the extreme temperature on the lower side. The relaxation time for the low temperature peak is represented as a function of the temperature in Fig. 13.

By using a thermodynamic fit according to the Eyring equation it is possible to obtain the activation enthalpy as well as the activation entropy and the Gibbs free energy (see Tables 2 and 3) for both processes under study. The relevant expression is

$$\tau(T) = \frac{2\pi h}{kT}\exp\frac{\Delta G^*}{kT}, \tag{15}$$

where $\Delta G^* = \Delta H^* - T\Delta S^*$.

A continuous increase of the Gibbs free energy with the temperature in both zones of relaxation is observed (see Tables 2 and 3).

It is interesting to note the negative values of the activation entropy for the low temperature peaks, as well as the significant values for the magnitude of this quantity in the 10–25°C range. These results indicate a very different character for the two relaxations. Also, note that the activation

Table 2
Thermodynamic coefficients

	T_p (°C)	T_m (°C)	ΔH^* (kcal mol^{-1})	ΔS^* (cal K^{-1} mol^{-1})	ΔG^* (kcal mol^{-1})
1	−120.0	−115.6	8.3367	−12.8574	10.3038
2	−110.0	−104.3	8.2111	−18.0542	11.1539
3	−100.0	−95.1	13.1652	8.8015	11.6426
4	−90.0	−85.8	13.2603	5.2039	12.3080
5	−80.0	−76.3	14.7798	9.4063	12.9644
6	−70.0	−66.3	17.5896	19.4066	13.6501

Table 3
Thermodynamic coefficients

	T_p (°C)	T_m (°C)	ΔH^* (kcal mol^{-1})	ΔS^* (cal K^{-1} mol^{-1})	ΔG^* (kcal mol^{-1})
1	10.0	17.1	49.1626	104.2148	19.6696
2	15.0	18.6	58.5540	135.3541	19.5720
3	20.0	22.4	65.9722	157.4386	19.8427
4	25.0	28.2	51.4633	104.0258	20.3646
5	30.0	31.8	35.9796	50.8130	20.5832
6	35.0	37.1	30.8406	32.7627	20.7497
7	40.0	61.6	37.7229	51.8946	21.4799

free energy (or enthalpy) at −80 or −70°C is close to the value obtained from dielectric a.c. measurements.

Summing up, there is evidence, through DSC, X-ray and a.c. dielectric relaxation measurements of a structural change near 70°C, involving a smectic C mesophase. It is well known that ferroelectric liquid cristal can be realized in smectic C phase by introducing a chiral carbon to reduce the symmetry, but ferroelectric modes (Goldstone and soft modes) are not observed in our experimental results. Perhaps because in our system they appear to be overlapped by the high loss in the low frequency side of the spectrum [13] or due the low level content of chiral entities is not enough to built the necessary helix.

Acknowledgements

This work was supported by the DGICYT through the grants MAT99-1127-C04-03 and MAT1998-0961-C02-01. One of us (A. G.-B.) thanks U.P.V. for a grant.

References

[1] Pérez E, Riande E, Bello A, Benavente R, Pereña JM. Macromolecules 1992;25:605.
[2] Pérez E, Benavente R, Bello A, Pereña JM, VanderHart DL. Macromolecules 1995;28:6211.
[3] Meyer RB, Liebert L, Strzelezcki L, Keller P. J Phys Paris Lett 1975;36:69.
[4] Kremer F, Vallerien SU, Zentel R. Adv Mater 1990;2(3):145.
[5] Illers KH, Breuer S. J Colloid Sci 1963;18:1.
[6] Díaz Calleja R, Sanchis MJ, Reiss-Nunes RC, Pinto M, Riande E. J Appl Phys 1995;78:1906.
[7] Havriliak S, Negami S. J Polym Sci 1967;14:99.
[8] Macdonald JR. Complex non linear least squares immitance fitting program LEVM6. Department of Physics and Astronomy, University of North Carolina, 1993.
[9] Williams G, Watts DG. Trans Faraday Soc 1970;66:80.
[10] Vogel H. Z Phys 1921;22:645.
[11] Fulcher GS. J Am Ceram Soc 1925;8:339.
[12] Tamman G, Hesse W. Z Anorg Allg Chem 1926;156:245.
[13] Vallerien SU, Kremer F, Scherowsky G, Schliwa A, Kuhnpast K, Fischer EW. Liq Cryst 1990;8(5):719.